Title
Persistence of Amygdala–Hippocampal Connectivity and Multi-Voxel Correlation Structures During Awake Rest After Fear Learning Predicts Long-Term Expression of Fear

Journal
Cerebral Cortex, 27(5)

ISSN
1047-3211

Authors
Hermans, Erno J
Kanen, Jonathan W
Tambini, Arielle
et al.

Publication Date
2017-05-01

DOI
10.1093/cercor/bhw145

Peer reviewed

Cerebral Cortex, May 2017;27:3028–3041

doi:10.1093/cercor/bhw145
Advance Access Publication Date: 30 May 2016

ORIGINAL ARTICLE

Persistence of Amygdala–Hippocampal Connectivity and Multi-Voxel Correlation Structures During Awake Rest After Fear Learning Predicts Long-Term Expression of Fear

Erno J. Hermans[1,3,4], Jonathan W. Kanen[1,5], Arielle Tambini[2,6], Guillén Fernández[3,4], Lila Davachi[1,2] and Elizabeth A. Phelps[1,2,7]

[1]Department of Psychology and [2]Center for Neural Science, New York University, New York, NY 10003, USA, [3]Donders Institute for Brain, Cognition and Behaviour and [4]Department for Cognitive Neuroscience, Radboud University Medical Centre, Nijmegen 6525 EN, The Netherlands, [5]Behavioural and Clinical Neuroscience Institute, Department of Psychology, University of Cambridge, Cambridge CB2 3EB, United Kingdom, [6]Helen Wills Neuroscience Institute, University of California, Berkeley, CA 94720, and [7]Nathan Kline Institute, Orangeburg, NY 10962, USA

Address correspondence to Erno J. Hermans, Donders Institute for Brain, Cognition and Behaviour, Centre for Cognitive Neuroimaging, PO Box 9101, 6500 HB Nijmegen, The Netherlands. Email: Erno.Hermans@donders.ru.nl

Abstract

After encoding, memories undergo a process of consolidation that determines long-term retention. For conditioned fear, animal models postulate that consolidation involves reactivations of neuronal assemblies supporting fear learning during postlearning "offline" periods. However, no human studies to date have investigated such processes, particularly in relation to long-term expression of fear. We tested 24 participants using functional MRI on 2 consecutive days in a fear conditioning paradigm involving 1 habituation block, 2 acquisition blocks, and 2 extinction blocks on day 1, and 2 re-extinction blocks on day 2. Conditioning blocks were preceded and followed by 4.5-min rest blocks. Strength of spontaneous recovery of fear on day 2 served as a measure of long-term expression of fear. Amygdala connectivity primarily with hippocampus increased progressively during postacquisition and postextinction rest on day 1. Intraregional multi-voxel correlation structures within amygdala and hippocampus sampled during a block of differential fear conditioning furthermore persisted after fear learning. Critically, both these main findings were stronger in participants who exhibited spontaneous recovery 24 h later. Our findings indicate that neural circuits activated during fear conditioning exhibit persistent postlearning activity that may be functionally relevant in promoting consolidation of the fear memory.

Key words: amygdala, fear conditioning, hippocampus, memory consolidation, ventromedial prefrontal cortex

Introduction

Although fear memories are rapidly acquired and highly persistent (Phelps 2004; Poulos et al. 2009), their long-term retention depends on a process of consolidation that transpires well beyond the learning experience (LaBar and Phelps 1998; McGaugh 2000). Animal models suggest a key role in this process for spontaneous reactivations of circuitry relevant for fear learning during offline periods such as sleep or awake rest (Paré 2003; Pape

and Paré 2010). However, no studies to date have investigated such processes in humans, particularly as they relate to the long-term expression of fear (Hermans et al. 2014).

The neural circuits underlying fear learning and expression comprise a set of strongly interconnected regions including amygdala, hippocampus, and prelimbic cortex (Pape and Paré 2010; Milad and Quirk 2012). Consolidation of emotional memory appears to depend particularly on the amygdala, which is thought to modulate synaptic plasticity in other brain regions (Roozendaal et al. 2009). Electrophysiological experiments in rodents have shown that theta synchronization between amygdala and hippocampus increases during acquisition and expression of conditioned fear (Seidenbecher et al. 2003), and that arousing experiences strengthen replay of waking patterns of hippocampal activity during postlearning rest periods (Karlsson and Frank 2009; Carr et al. 2011). Furthermore, amygdala–hippocampal theta synchronization is increased during sleep after fear learning and predicts fear retention 1 day later (Popa et al. 2010), suggesting a role in consolidation of fear memory.

In contrast, extinction learning relies on circuits involving infralimbic cortex (or its putative human homolog, ventromedial prefrontal cortex; vmPFC) (Milad and Quirk 2002). Extinction establishes a competing safety memory and does not replace the original fear memory (Bouton 2002; Dunsmoor et al. 2015). Extinguished fear can therefore return, for instance, with passage of time (spontaneous recovery) or after re-exposure to unconditioned stimuli (reinstatement). These observations suggest that consolidation of the original fear memory may proceed despite the fact that the expression of this memory is inhibited following extinction.

In humans, functional connectivity methods using blood oxygenation level-dependent functional magnetic resonance imaging (BOLD-fMRI) may allow investigation of spontaneous neural interactions underlying consolidation. Specifically, it is possible that immediate post-encoding time periods allow for the initial stages of memory consolidation to unfold. Patterns of functional connectivity during awake rest, for instance, show signatures of recently performed tasks within 5–15 min time windows. Such effects have been shown for numerous cognitive domains, including motor learning (Albert et al. 2009), visual perception (Lewis et al. 2009), language comprehension (Hasson et al. 2009), spatial navigation (Wegman and Janzen 2011), emotional arousal (van Marle et al. 2010), and classical conditioning (Schultz et al. 2012; Feng et al. 2013). Recent studies furthermore demonstrated that hippocampal–neocortical connectivity persists during rest following memory encoding (Tambini et al. 2010; van Kesteren et al. 2010). Persistence of this connectivity (Tambini et al. 2010) as well as hippocampal (Tambini and Davachi 2013) and entorhinal (Staresina et al. 2013) activity patterns during postencoding rest predict subsequent memory. We therefore hypothesized that increased functional connectivity following fear learning within the circuits outlined above would predict long-term expression of these fear memories when tested after a period of consolidation.

The basal and lateral subregions of the amygdala are critical sites of neural plasticity underlying fear learning (Miserendino et al. 1990; Rogan et al. 1997). In these areas, fear associations are thought to be sparsely coded across distributed neuronal assemblies that respond to particular conjunctions of sensory information (Reijmers et al. 2007). Although BOLD-fMRI in humans cannot spatially resolve activation of individual neurons, activation of specific distributed neuronal assemblies can be detected using pattern recognition techniques applied across large sets of voxels (Bach et al. 2011; Rissman and Wagner 2012). We reasoned that if neuronal assemblies within the amygdala that represent a fear memory reactivate spontaneously during offline periods following learning, then multi-voxel activity patterns sampled during fear learning should re-emerge spontaneously during these periods. We further hypothesized that such an effect would also be associated with long-term expression of this fear memory.

To test our hypotheses, 24 participants underwent fMRI on 2 consecutive days during a fear conditioning paradigm (Fig. 1) consisting of 1 habituation block, 2 acquisition blocks, and 2 extinction blocks on day 1, and 2 re-extinction blocks on day 2. During acquisition, one of 2 photographs of faces (CS+) coterminated with mild electrical shock (unconditioned stimulus; US) on 50% of CS+ trials, while the other (CS–) was never paired with shock. The differential conditioned anticipatory pupil dilation response (CR) between CS+ and CS– served as a measure of conditioned fear (Fig. 2). No shocks were given during habituation,

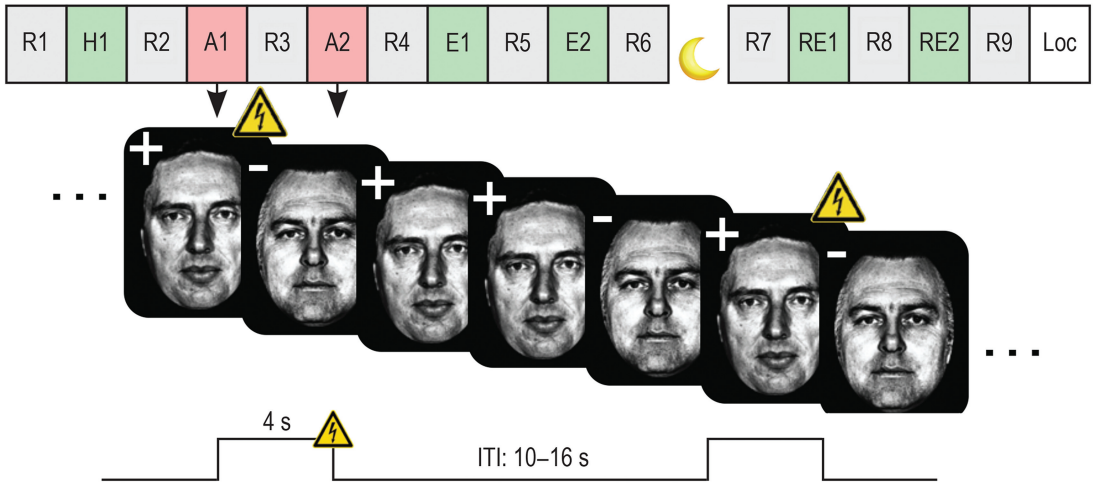

Figure 1. Design overview. Conditioning blocks were intermixed with resting-state blocks (4.5 min each) on 2 consecutive days. Two stimuli (CS+/CS–) were shown in pseudorandom order during conditioning blocks (16 CSs/block). CS+s coterminated with shock on 50% of acquisition trials. R1–9, rest blocks; H1, habituation; A1–2, acquisition; E1–2, extinction; RE1–2, re-extinction, Loc, localizer task; ITI, intertrial interval.

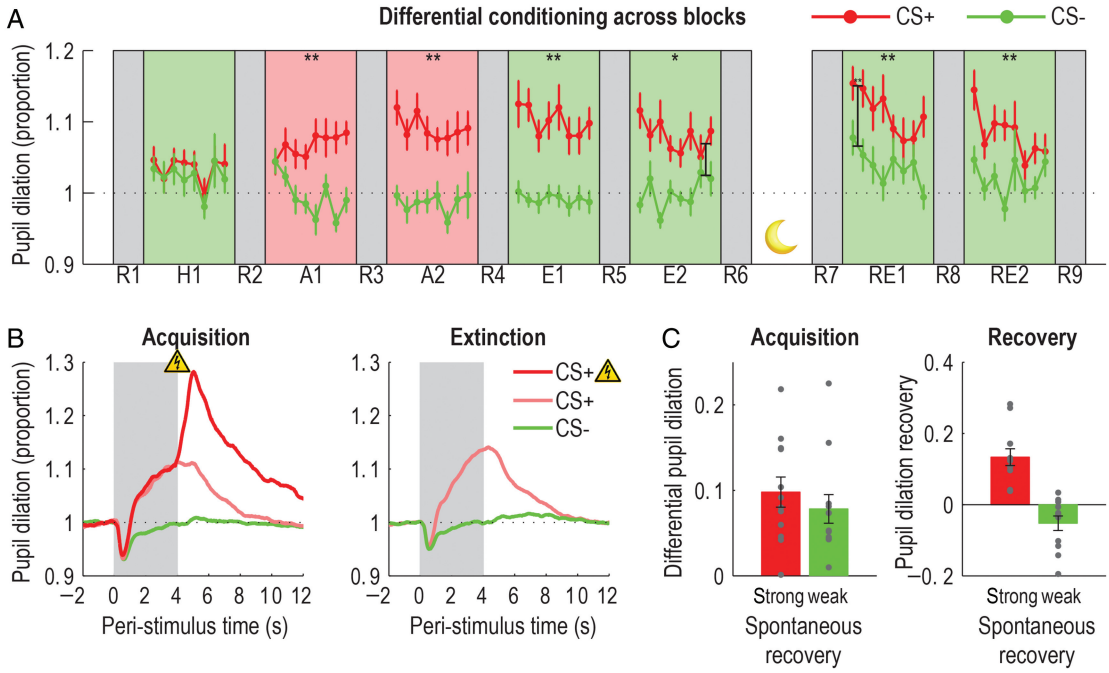

Figure 2. Conditioned pupil dilation. (*A*) Pupil dilation response magnitudes to CS+ and CS− trials across 2 days. The increase in differential response from the last 2 CS+/CS− extinction trials on day 1 and the first 2 re-extinction trials on day 2 served as an index of spontaneous recovery. (*B*) Averaged (across all trials and participants) event-related pupil dilation responses during acquisition and extinction for reinforced CS+ trials, unreinforced CS+ trials, and CS− trials. CS duration is indicated by a gray rectangle. (*C*) Differential conditioned responses during acquisition and strength of spontaneous recovery on day 2 separated for participants exhibiting strong versus weak spontaneous recovery. Note that groups are defined using a median split across this spontaneous recovery measure. R1–9, resting-state blocks; H1, habituation; A1–2, acquisition; E1–2, extinction; RE1–2, re-extinction 1–2; $^{*}P < 0.001$; $^{**}P < 0.0001$. All error bars indicate standard error of the mean.

extinction, and re-extinction. On day 2, we assessed spontaneous recovery of fear (an increase in differential CR from the end of day 1 extinction to the beginning of day 2 re-extinction). 4.5-min CS presentation blocks were preceded and followed by 4.5-min awake rest blocks. We functionally defined the face-responsive region of the fusiform gyrus (fusiform face area, FFA; a region involved in identifying the facial CSs; Kanwisher et al. 1997) using an independent localizer. Primary visual cortex was included as a control region of interest (ROI).

We predicted that resting functional connectivity between the amygdala and other regions known to be involved in fear conditioning would increase from baseline following acquisition and could persist after extinction. Within the amygdala, we expected that if neuronal assemblies involved in fear learning reactivate spontaneously during postlearning rest, this would result in a structure of voxel-pairwise correlations during postlearning rest that resembles the correlation structure observed during fear learning. This multi-voxel correlation structure (MVCS) approach (Tambini and Davachi 2013) is based on techniques used in rodent electrophysiology to investigate replay (Qin et al. 1997; Kudrimoti et al. 1999). Finally, we expected that both these effects would be linked to long-term expression of the fear memory, which would be reflected in greater spontaneous recovery of fear on subsequent days.

Materials and Methods

Participants

Twenty-four healthy right-handed participants with normal or corrected-to-normal vision completed the study (12 females, 12 males). Ages ranged from 18 to 36 (mean: 22.8 years). Volunteers had never participated in a fear conditioning study and were screened for psychiatric and neurological medication. Participation of 7 additional individuals was terminated for various reasons (apparatus failure, falling asleep, or noncompliance with instructions). All participants received financial compensation. The protocol was approved by the University Committee on Activities Involving Human Subjects (UCAIHS) at New York University, and all participants provided informed consent before the experiment.

Based on measures of spontaneous recovery of fear on day 2 (explained under "Fear conditioning paradigm" below), participants were divided into 2 groups. These groups did not differ in age ($F < 1$, n.s.), Spielberger's Trait Anxiety Inventory scores (STAI: $F < 1$, n.s.), Beck Depression Inventory scores ($F < 1$, n.s.), gender distribution ($\chi^2 = 2.67$, n.s.), or time of testing ($F < 1$, n.s.; note that participants were tested on the same time of day for both sessions). We did not acquire objective data on sleep quality and quantity. The possibility that there is a systematic variation in sleep quality between groups, although unlikely, could therefore not be ruled out.

Design and Procedure

Participants were tested on 2 consecutive days (Fig. 1). In a staircase procedure, participants chose individual shock levels that they considered uncomfortable, but not painful. In the scanner, participants underwent a differential delay fear conditioning paradigm comprising 1 habituation block, 2 acquisition blocks, and 2 extinction blocks on the first day. Twenty-four hours later participants returned for a test of spontaneous recovery in 2 identical (re-) extinction blocks. On both days, each of these conditioning blocks was preceded and followed by a resting-state

block. All blocks had a 4.5-min duration. Scanning on day 2 concluded with an FFA localizer task and a high-resolution anatomical scan. Participants wore ear plugs, and head movement was restricted using foam pads. Stimuli were back-projected onto a translucent screen positioned behind the participant's head that was visible through a mirror mounted on the head coil. The scan room was darkened. Stimuli were presented using E-Prime (Psychology Software Tools, Inc., Pittsburgh, PA, USA). We administered personality (STAI and BDI) and contingency awareness questionnaires after scanning.

Fear Conditioning Paradigm

Each conditioning block comprised 8 presentations of each of the 2 stimuli (CS+/CS−). Each CS was presented for 4 s, with random intertrial intervals (ITIs; gray screen with fixation cross) ranging from 10 to 16 s. During acquisition blocks, the CS+ coterminated with an unconditioned stimulus (US; mild electrical shock) on 50% of trials (total: 8 shocks across 2 blocks). Partial reinforcement was used to avoid rapid extinction (LaBar et al. 1998). The CS− was never paired with shock. Stimulus order was pseudorandomized such that no stimulus type was presented on >3 consecutive trials. We used 2 gray-scaled facial stimuli selected from the Karolinska Directed Emotional Faces (Lundqvist et al. 1998). Each served as CS+ in 50% of participants. To ensure that pupil dilation cannot be attributed to luminance differences, mean luminance of the CSs, background, and ITI fixation-cross screen was equalized. All other conditioning blocks (habituation, extinction, re-extinction) were identical to acquisition blocks but lacked reinforcement. Participants were instructed that they would see 2 images, and that one of them may sometimes be paired with a shock. On day 2, instructions were that the procedure would continue with identical settings, including the shock level set on day 1 (in reality, no shocks were delivered on day 2). The increase in the differential conditioning effect (CS+ > CS−) from the last 2 pairs of trials on day 1 to the first 2 pairs of trials on day 2 was used as a measure of spontaneous recovery (cf. Hartley et al. 2011).

Resting-State Blocks

Rest blocks (4.5-min duration) were interleaved with conditioning blocks throughout the experiment (Fig. 1) to allow for assessment of postacquisition and postextinction changes in intrinsic activity. Throughout these blocks, a black screen with a dark green fixation cross was presented. Participants were instructed to remain awake and alert, keep their eyes open, let their mind wander freely, and avoid repetitive mental activity such as counting (see Van Dijk et al. 2010). We verified compliance with the instruction to remain awake using eye tracking.

FFA Localizer

A 2-category localizer was used to individually identify face-responsive regions in the fusiform gyrus (FFA). This task consisted of 4 blocks of 24 faces, alternated with 4 blocks of 24 scrambled faces. Each stimulus was presented with 1 s duration (total 24 s/block). A small red dot appeared in the center of 1 stimulus in each block. Participants were instructed to pay attention to all stimuli and to indicate, using right index finger button presses, when red dots appeared. Scrambled faces were created by randomly scrambling the phase information of each of the 24 photographs after 2D Fourier transform (Reinders et al. 2005).

Peripheral Stimulation and Measurements

Mild electric shocks were delivered through a bar electrode attached to the inner wrist using a Velcro strap. We used a Grass Technologies (West Warwick, RI, USA) SD9 Stimulator charged by a stabilized current. Half of the participants received shock on the right wrist, half on the left. Each shock had a 200-ms duration and consisted of a 50-Hz block pulse. Shocks were individually set between 20 and 60 V (mean: 36).

Pupil diameter was measured using an EyeLink 1000 eye-tracking system (SR Research, Kanata, Ontario, Canada). The system included an infrared videographic camera equipped with a telephoto lens, which was focused on the right eye through a flat surface mirror mounted on the RF coil. Pupil data were analyzed using in-house software (Hermans et al. 2013) implemented in Matlab 7.9 (The Mathworks, Natick, MA, USA). Eye blink artifacts were identified automatically and removed using linear interpolation (Siegle 2003). Event-related pupil dilation responses were calculated by dividing averaged pupil diameter during the 1 to 4 s period after CS onset by the averaged 1 s prior to onset. This period was chosen to avoid the confounding influence of the initial light reflex (a parasympathetically regulated pupil constriction) upon stimulus onset. We used pupil dilation as our main dependent measure to assess conditioned fear, because pupil dilation responses can, unlike skin conductance responses (SCRs), be measured before shock delivery on reinforced CS+ trials (Reinhard and Lachnit 2002). We assessed the reliability of skin conductance and pupil dilation measures across sessions by computing Spearman's rank-order correlation coefficients (to accommodate skewness in SCR data) between mean response magnitudes collapsed across trial types on day 1 and those on day 2, for both measures (see Results section).

Skin conductance, heart rate, and respiration measures were recorded at 200 Hz using a BIOPAC Systems (Santa Barbara, CA, USA) MP100 acquisition system. SCR was recorded through Ag-AgCl electrodes attached to the distal phalanges of the index and middle fingers of the hand opposite the shock electrode. SCRs to CSs and USs were scored offline using AcqKnowledge 3.9 software (BIOPAC Systems) by determining the base-to-peak difference for the first waveform (in μSiem) in the 0.5–4.5 s window after stimulus onset. SCR magnitudes were square root transformed to normalize distributions.

Pulse was recorded using a pulse oximeter transducer affixed to the fourth or fifth finger of the hand opposite the shock electrode. Respiration was measured using a respiration belt placed around the participant's abdomen. Pulse and respiration measures were used for retrospective image-based correction (RETROICOR) of physiological noise artifacts in BOLD-fMRI data (Glover et al. 2000). Raw pulse and respiratory data were processed offline using in-house software for interactive visual artifact correction and peak detection, and were used to specify fifth order Fourier models of the cardiac and respiratory phase-related modulation of the BOLD signal, yielding 10 nuisance regressors for cardiac noise and 10 for respiratory noise. Additional regressors were calculated for heart rate frequency, heart rate variability, (raw) abdominal circumference, respiratory frequency, respiratory amplitude, and respiration volume per unit time, yielding a total of 26 RETROICOR regressors.

MRI Data Acquisition

MRI scans were acquired using a 3 T Siemens (Erlangen, Germany) Allegra head-only scanner equipped with a Nova Medical head coil. T_2^*-weighted BOLD images were recorded using a customized

multi-echo EPI sequence (TR: 2160 ms, flip angle: 90°, FOV: 240 × 192 mm, 37 ascending slices, 2.8 mm slice thickness, 0.28 mm slice gap, bandwidth: 4166 Hz/px, echo spacing: 0.31 ms) with 3 echoes following each RF pulse: a low resolution image (TE: 7.56 ms, matrix: 80 × 16), a full resolution partial-Fourier (6/8) image (TE: 12.2 ms, reversed phase encoding gradients, matrix: 80 × 64), and a fully sampled image (TE: 32.4, matrix: 80 × 64). This sequence mitigates susceptibility artifacts in medial temporal and vmPFC regions by determining weighted averages of signal across the readout and correcting for susceptibility-related image deformation using the reverse phase-encoding gradients image (cf. Andersson et al. 2003). In total, 1382, 632, and 96 volumes were acquired continuously for conditioning day 1, conditioning day 2, and the FFA localizer, respectively.

T_1-weighted structural scans were obtained using an MP-RAGE sequence with the following parameters: TE/TR: 3.93/2500 ms, flip angle: 8°, FOV: 256 × 256 × 176 mm, voxel size: 1 mm isotropic.

MRI Data Spatial Preprocessing

MRI data recorded during conditioning blocks were preprocessed for general linear model (GLM)-based analyses in standard stereotactic (MNI152) space using SPM8 (http://www.fil.ion.ucl.ac.uk/spm). Motion correction was performed on all functional scans using a rigid body transformation and sum of squared differences minimization. We verified that averaged measures of scan-to-scan 3-dimensional movement (Thomason et al. 2005) did not differ between groups of participants exhibiting strong versus weak spontaneous recovery on day 2. Mutual information maximization-based rigid body registration was used to register functional and structural images. Structural images were segmented into gray matter, white matter, and CSF images using a unified probabilistic template registration and tissue classification method (Ashburner and Friston 2005). Using DARTEL (Ashburner 2007), gray and white matter images of all 24 participants were combined to produce a template image, which in turn was registered (using an affine transformation) with the MNI152 template included in SPM8. Identical transformations were applied to functional images, which were resliced into 2 mm isotropic voxels and smoothed with a 6 mm FWHM Gaussian kernel.

For interregional and intraregional analyses of functional connectivity, MRI data recorded were preprocessed in native space using motion correction, coregistration between functional and structural scans, and reslicing into 2-mm isotropic voxels without smoothing.

Statistical Analysis of Event-Related BOLD Responses to CS Presentations

For whole-brain event-related analyses, GLMs were specified for each phase of the conditioning paradigm (habituation, acquisition, extinction, re-extinction). BOLD responses to CS+s and CS−s were modeled in 2 separate regressors using 4-s box functions. For the acquisition phase, responses to reinforced CS+s and USs were modeled in separate regressors. First- and second-order time modulation regressors were added for each to model habituation of responses. Task regressors were temporally convolved with the canonical SPM8 hemodynamic response function. Models additionally included 6 movement parameter regressors (3 translations, 3 rotations) derived from rigid body motion correction, 26 RETROICOR physiological noise regressors, high-pass filtering (1/128 Hz cutoff), and AR(1) serial correlations correction. Single-subject parameter estimates for CS+s and CS− response magnitudes obtained from first-level analyses were entered into group-level random effects (RFX) analyses using factorial ANOVAs with CS (CS+ vs. CS−) and block (first vs. second; for acquisition, extinction, and re-extinction only) as within-subject factors. Alpha was set at 0.05; whole-brain family-wise error (FWE) corrected using Gaussian Random Field Theory-based methods. Based on a priori hypotheses, results for amygdala and hippocampus are corrected for reduced search volumes using small volume corrections based on anatomical masks (Automated Anatomical Labeling atlas; Tzourio-Mazoyer et al. 2002).

ROI Definition and Data Extraction for Native Space Connectivity Analyses

Amygdala and hippocampus ROIs were defined using individual anatomical segmentation of T_1-weighted images (see Supplementary Fig. 1) using FSL FIRST (http://www.fmrib.ox.ac.uk/fsl/first/index.html). Data from the localizer task were used to create native space functional ROIs of the FFA. BOLD-fMRI data were preprocessed in native space identical to the resting-state blocks but with additional smoothing using a 6 mm FWHM Gaussian kernel. A GLM model was used that included a task regressor coding for the difference between face and scrambled face blocks and all nuisance regressors used in the conditioning blocks analyses. Bilateral FFA peaks were defined as the most responsive voxels in the left and right fusiform gyrus for the face > scrambled face contrast (Kanwisher et al. 1997). ROIs were then defined as the 75% most responsive voxels within a 6 mm radius from this peak. We also used a functional definition for the vmPFC. The vmPFC has consistently been implicated in extinction learning in humans (Phelps et al. 2004). We therefore used the group-level peak coordinate (i.e., [8, 52, −10], see Supplementary Table 2, in the medial/orbital region below the subgenual ACC) derived from the CS− > CS+ contrast in the vmPFC during the combined extinction blocks on day 1. The DARTEL-generated spatial normalization parameters were applied in a reverse fashion to transfer these MNI space coordinates back to native space. Subsequently, all voxels within a 6 mm radius sphere around this location were included in the vmPFC ROI. We furthermore included an ROI for the dACC, which is implicated in fear expression (Milad and Quirk 2012), This ROI was based on the group-level peak coordinate (i.e., [4, 12, 44], see Supplementary Table 1) for the CS+ > CS− contrast during acquisition. To define a control ROI, we used an identical procedure for the peak voxel in the CS > baseline contrast during acquisition, yielding an ROI around a peak voxel (at [−6, −84, −10]) at the edge of V1 (BA17/18). BOLD-fMRI time series were extracted from each voxel, region (5), hemisphere (2), and 4.5-min block (9 resting-state blocks). Before further analysis, we used a multiple regression model to remove nuisance signals from each time course through residualization. This model included a high-pass filter (1/128 Hz), 6 movement parameter regressors (3 translations, 3 rotations), and 26 RETROICOR physiological noise regressors.

Interregional Functional Connectivity MRI Analyses

To investigate alterations in functional connectivity across blocks between our regions of interest, BOLD-fMRI voxel time courses were averaged for each ROI, hemisphere, and block. Functional connectivity between regions was calculated using pairwise Pearson correlation coefficients between regions (see Fig. 3B). Pearson correlation coefficients were Fisher's z-transformed to normalize distributions using the following formula:

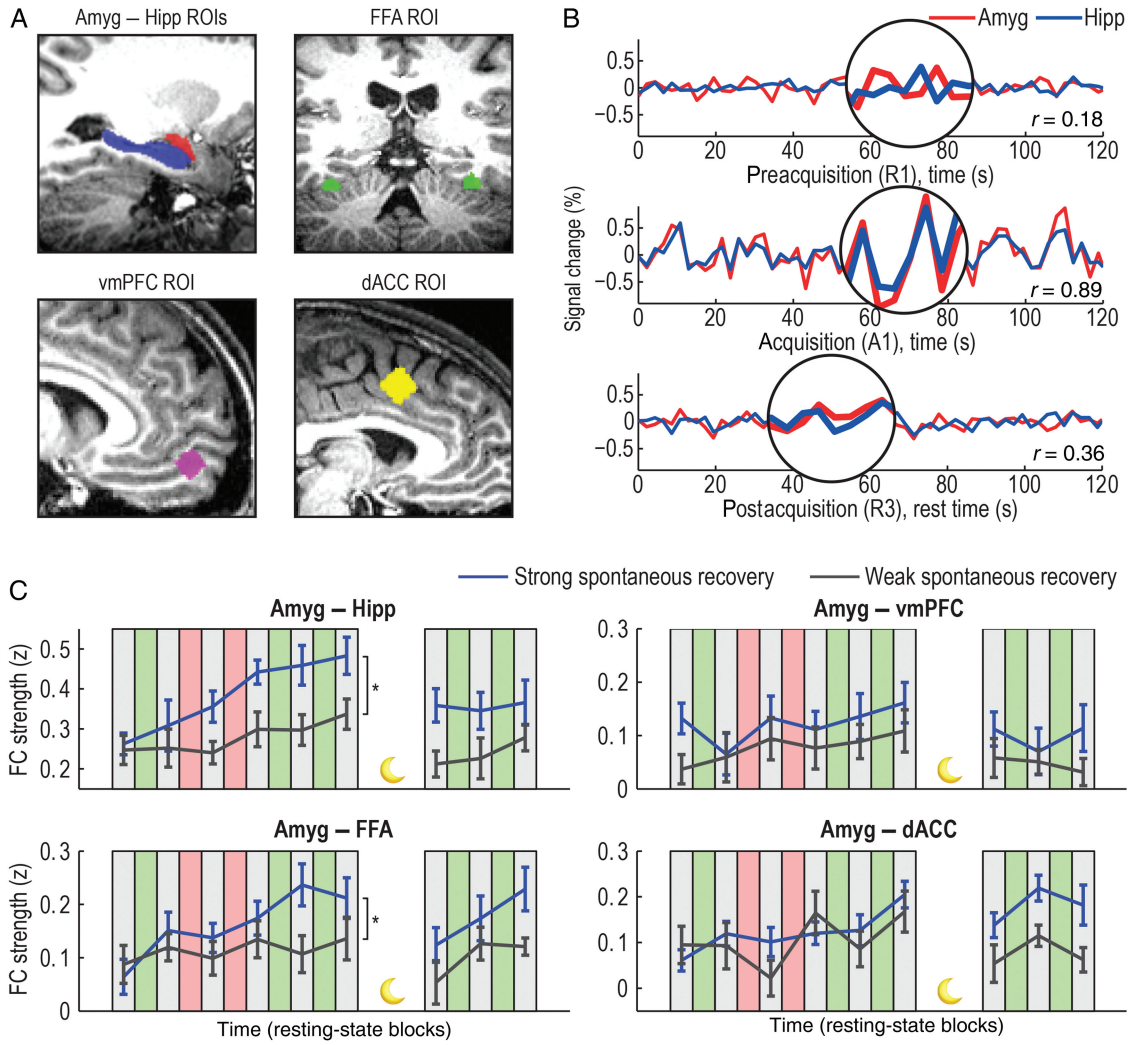

Figure 3. Functional connectivity analyses. (*A*) Illustration of ROIs. Amygdala (red) and hippocampus (blue) were delineated using segmentation of individual structural scans. FFA (green) was defined functionally using a separate localizer task. vmPFC (violet) was defined as a spherical region surrounding the peak voxel of the differential response during extinction. dACC (yellow) was defined as a spherical region surrounding the peak voxel for the CS+ > CS− contrast during acquisition. (*B*) Illustration of changes in functional connectivity between the amygdala and hippocampus from before to after fear conditioning. Data shown are from a single participant and depict the first 2 min of each block. During preacquisition rest, the smallest correlation between time courses is observed. During acquisition, stimulus presentation causes activity to synchronize (see Supplementary Fig. 3). Finally, a stronger connectivity is preserved during postacquisition rest. (*C*) Functional connectivity of the amygdala with the other 4 ROIs during resting-state blocks (R1–9). Background boxes indicate order of resting (gray) and CS presentation blocks (red/green). Separate traces are shown for participants who exhibit strong spontaneous recovery of conditioned fear on day 2 and those that show weak recovery. ROI, region of interest; Amyg, amygdala; Hipp, hippocampus; FFA, fusiform face area; vmPFC, ventromedial prefrontal cortex; dACC, dorsal anterior cingulate cortex; FC, functional connectivity; $^*P < 0.05$.

$z = 0.5[\log_e((1 + r)/(1 - r))]$ (Tambini et al. 2010; van Kesteren et al. 2010). Resulting z values were analyzed using repeated-measures ANOVAs with block and hemisphere as within-subject factors and spontaneous recovery as between-subjects factor. Effects involving the spontaneous recovery factor (based on median split) were corroborated using Spearman's rank order correlations of spontaneous recovery strength with the relevant difference scores. These additional analyses are reported in the Supplementary Results.

Intraregional Multi-Voxel Correlation Structure Analyses

Within-region correlation structures were analyzed using a method derived from rodent electrophysiology to quantify reactivations of distributed neuronal assemblies (Qin et al. 1997; Kudrimoti et al. 1999; Lansink et al. 2008). Within each region, we calculated Pearson's correlations between each of *n* BOLD-fMRI voxel time courses, yielding an *n* by *n* MVCS matrix consisting of pairwise correlations. This procedure was repeated for each hemisphere and 4.5-min block, for both amygdala and hippocampus. Because the MVCS is symmetrical, further calculations were done on values below the diagonal. If a specific learning experience is encoded in the simultaneous activation of a sparsely distributed assembly of voxels within a region (Bach et al. 2011), then reactivation of this memory trace should lead to the reinstatement of a specific pattern within the MVCS. The reason for this is that simultaneous activation of a specific set of voxels 1) in response to stimuli or 2) spontaneously would both lead to enhanced correlations between the time courses of these voxels in the MVCS. Thus, a significant proportion of the variance across elements in the MVCS sampled during postlearning rest would then be explained by variance measured during learning, even

when controlling for any preexisting covariance (e.g., reflecting underlying structural connectivity patterns). To test this, we computed the partial correlation between the MVCS matrices sampled during acquisition of conditioned fear (Fig. 1: block A1) and each resting-state block following acquisition (block R3–6 for day 1, R7–9 for day 2), while factoring out variance explained by the MVCS sampled during baseline rest (block R1). Analogous to rodent studies, this partial correlation was squared to obtain a measure of the explained variance (EV; Kudrimoti et al. 1999). To obtain a within-subject control measure, we also computed the reverse explained variance (REV; see Lansink et al. 2008), in which the resting-state blocks before and after learning are exchanged (see Fig. 4). Evidence of reactivation for a specific block of postlearning rest is obtained if EV > REV. Measures of EV and REV were entered into repeated-measures ANOVAs with EVvsREV, block, and hemisphere as within-subject factors and spontaneous recovery as between-subjects factor. Effects involving the (median split-based) spontaneous recovery factor were again corroborated using Spearman's rank order correlations and reported in the Supplementary Results.

Note that because the time interval between the first acquisition block (A1) and all resting blocks after R3 is equal to or larger than the time interval between A1 and the baseline rest block (R1), persistence of MVCSs (EV > REV) from A1 to these rest blocks cannot be explained by autocorrelation of the BOLD signal.

Statistical Testing

For repeated-measures ANOVAs in which sphericity assumptions were violated as indicated by Mauchly's test, Greenhouse–

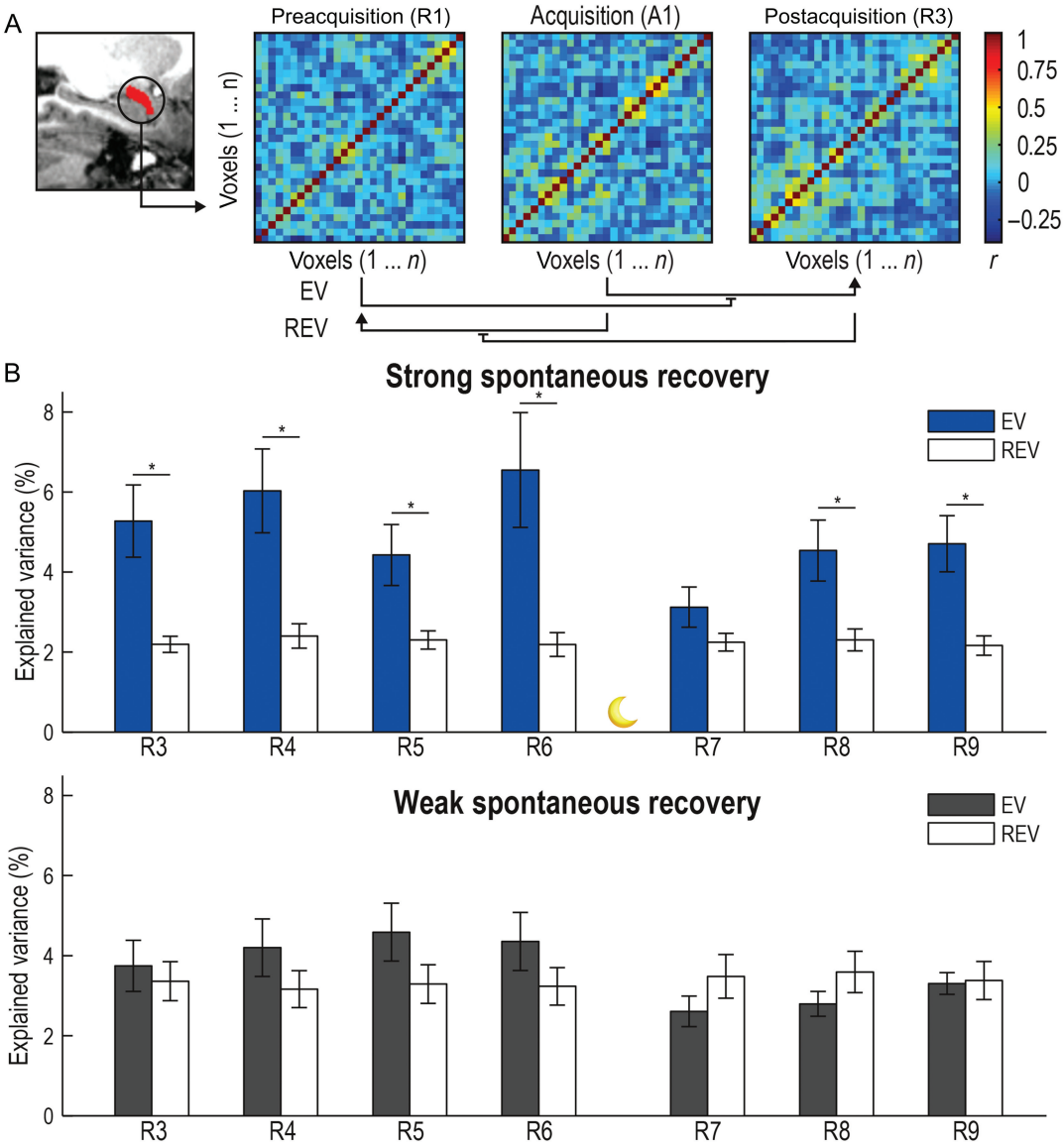

Figure 4. Intraregional multi-voxel connectivity structure (MVCS) analysis on the amygdala. (*A*) Example MVCSs (pairwise correlation matrices) of the left amygdala for 1 participant. EV (explained variance) is calculated as the proportion of variance in the MVCS sampled postacquisition that is explained by the MVCS sampled during acquisition, while controlling for variance in the preacquisition MVCS. For REV (reverse explained variance), pre- and postacquisition measures are exchanged. Evidence for reinstatement of connectivity patterns during rest following learning is obtained when EV > REV. (*B*) EV and REV are plotted for bilateral amygdala, separately for each resting-state block after fear learning (R3–9) and group (strong spontaneous recovery vs. weak spontaneous recovery); *$P < 0.05$.

Geisser Epsilon (GGε) corrections were applied. Partial squared ($P\eta^2$) effect size estimates are reported for all tests. Alpha was set at 0.05 throughout.

Results

Physiological Measures

We observed robust differential conditioned pupil dilation throughout acquisition [$t_{(23)} = 7.30$, $P = 2E{-}7$], extinction [$t_{(23)} = 6.00$, $P = 4E{-}6$], and re-extinction [$t_{(23)} = 5.76$, $P = 7E{-}6$], but not during habituation [before conditioning; $t_{(23)} = 1.49$, n.s.; Fig. 2]. Differential pupil conditioning was nonsignificant by the end of day 1 extinction [last 2 CS+ > last 2 CS−: $t_{(23)} = 1.48$, n.s.] but significant at the beginning of day 2 [first 2 CS+ > first 2 CS−: $t_{(23)} = 5.0$, $P = 4E{-}5$]. Nonetheless, the increase in differential conditioning on day 2 (i.e., the differential conditioning effect at the beginning of day 2 minus the differential conditioning effect at the end of day 1 extinction) did not reach significance across the entire participant sample [$t_{(23)} = 1.65$, $P = 0.113$], suggesting that differential fear responding recovered spontaneously in only a subset of participants. We therefore reasoned that this increase in differential responding can be used as an index of fear memory retention strength (cf. Hartley et al. 2011). This measure did not correlate with the differential response during acquisition [$r(22) = 0.07$, n.s.] and therefore does not simply reflect strength of initial learning. Furthermore, neither heart rate during rest blocks nor heart rate during conditioning blocks correlated with spontaneous recovery [all $r(22) < 0.2$, n.s.], indicating that spontaneous recovery is also not explained by general arousal around the time of learning. To distinguish a group of participants who show strong recovery from a group that does not, MRI data below are analyzed with a median split across strength of spontaneous recovery of differential conditioned pupil dilation as between-subjects variable (Fig. 2).

SCRs revealed a pattern that was similar to pupil dilation. Robust differential SCRs were seen throughout acquisition [$t_{(23)} = 7.42$, $P = 2E{-}7$], extinction [$t_{(23)} = 6.00$, $P = 4E{-}6$], and re-extinction [$t_{(23)} = 5.76$, $P = 7E{-}6$], and we also found no overall increase in differential responding from the end of extinction on day 1 to the beginning of re-extinction of day 2 [$t_{(23)} = -0.63$, n.s.]. However, SCRs showed more variability than pupil dilation responses, particularly regarding the stability across the 2 days. While averaged pupil dilation responses across trial types were strongly correlated between days [$\rho_{(22)} = 0.81$, $P = 1.7E{-}6$], SCRs were not [$\rho_{(22)} = 0.30$, n.s.]. Conditioned pupil dilation is therefore a more reliable measure to compare fear responses across days. We therefore used a median split across strength of spontaneous recovery of differential conditioned pupil dilation as a between-subjects variable in MRI analyses.

Event-Related BOLD Responses to CS Presentations

We first verified that our main ROIs exhibited the expected event-related activation in response to CS presentations using conventional group analyses in standard stereotactic (MNI152) space. Replicating earlier work (Phelps et al. 2004), we observed robust differential BOLD responses (CS+ > CS−) during acquisition in the amygdala (peak $t = 4.18$, $P < 0.05$, small volume corrected [SVC]) and hippocampus (peak $t = 5.22$, $P < 0.005$, SVC), but also in dorsal ACC, anterior insula, and temporoparietal junction, among other regions (see Supplementary Table 1). Neither differential BOLD responses in the amygdala (peak $t = 1.35$, $P = 0.96$, SVC) nor in the hippocampus (peak $t = 2.05$, $P = 0.99$, SVC) predicted spontaneous recovery of fear on day 2. During extinction (see Supplementary Table 2), we found a cluster within the vmPFC that showed a greater BOLD response to the CS− than to the CS+ (see Phelps et al. 2004). This cluster peaked just below the subgenual ACC ($t = 6.01$, $P < 0.005$, whole-brain corrected). Ventromedial PFC activity did not predict reduced spontaneous recovery on day 2 (peak $t = 0.78$, n.s.). Differential BOLD responses (CS+ > CS−) in amygdala and hippocampus diminished during extinction but recovered during re-extinction on day 2 (see Supplementary Table 3; amygdala: $t = 4.53$, $P < 0.005$, SVC; hippocampus: $t = 4.97$, $P < 0.005$, SVC). These differential BOLD responses were unrelated to physiological measures of spontaneous recovery of fear.

Interregional Functional Connectivity During Habituation, Acquisition, and (Re)-extinction Blocks

We then examined whether functional connectivity between the amygdala and our other ROIs (hippocampus, vmPFC, dACC, FFA, and V1; see Fig. 3A) changed across the 4.5-min blocks of habituation, acquisition, and (re)-extinction. All these ROI analyses were performed without stereotactic normalization to increase specificity. After delineating each ROI, BOLD signal time courses were extracted and averaged separately for each ROI and 4.5-min block. Subsequently, interregional Fisher z-transformed pairwise correlation coefficients were computed as a measure of functional connectivity strength. As expected, we found task-driven increases from baseline (block R1) in correlated activity between the amygdala and all other ROIs ($P < 0.05$) except dACC (see Supplementary Fig. 2). Indicating that amygdala involvement is particularly crucial during learning, these increases generally peaked during the early acquisition phase and then followed a downward trend back to baseline. Amygdala connectivity with none of our ROIs was associated with spontaneous recovery of conditioned fear on day 2 [for hippocampus, vmPFC, and V1: all $F < 1$, n.s.; for dACC: $F_{1,\ 22} = 2.00$, n.s.; for FFA: $F_{1,\ 22} = 2.68$, n.s.].

Interregional Functional Connectivity During Awake Rest Blocks

The first analysis of primary interest examined whether increased functional connectivity of the amygdala with other ROIs persisted during resting-state blocks following acquisition and extinction. Functional connectivity strengths of resting-state blocks on day 1 were entered into rmANOVAs with time (block 1–6) and hemisphere (left vs. right) as within-subject factors. For amygdala connectivity with hippocampus, we observed a main effect of block [$F_{5,\ 115} = 7.43$, $P < 0.001$, $P\eta^2 = 0.24$] with a linear trend [$F_{1,\ 23} = 26.49$, $P < 0.001$, $P\eta^2 = 0.54$], indicating a gradual increase of functional connectivity across day 1 resting-state blocks (including postacquisition and postextinction). Similar but weaker linear increases were found for amygdala connectivity with FFA [$F_{1,\ 23} = 12.17$, $P = 0.002$, $P\eta^2 = 0.35$], dACC [$F_{1,\ 23} = 15.85$, $P < 0.001$, $P\eta^2 = .41$], V1 [$F_{1,\ 23} = 13.31$, $P = 0.001$, $P\eta^2 = 0.37$], and vmPFC [$F_{1,\ 23} = 4.16$, $P = 0.053$, $P\eta^2 = 0.15$]. Amygdala connectivity with hippocampus [$F_{1,\ 22} = 12.15$, $P = 0.002$, $P\eta^2 = 0.36$] and FFA [$F_{1,\ 22} = 7.64$, $P = 0.011$, $P\eta^2 = 0.26$] was significantly increased already during postacquisition rest (block R3–4 vs. R1). No differences were found between baseline measures of functional connectivity on day 1 (R1) and day 2 (R7; $F < 1$, n.s., for all ROIs). Thus, unlike downward trends observed during CS presentation blocks, resting-state amygdala connectivity with other ROIs, in particular hippocampus, increased over time on day 1, persisted after extinction learning, and returned to baseline on day 2.

Next, we asked whether this gradual increase in functional connectivity of the amygdala following acquisition was related

to spontaneous recovery of fear on day 2. To answer this question, we entered the median split variable (indicating strong vs. weak spontaneous recovery) as a between-subjects variable into rmANOVAs of resting-state functional connectivity blocks. Critically, we found a progressive differentiation between the 2 groups [block × group linear trend: $F_{1,\ 22} = 6.20$, $P = 0.021$, $P\eta^2 = 0.22$], with participants who exhibit strong spontaneous recovery showing a stronger increase in amygdala–hippocampal connectivity following acquisition [$F_{1,\ 22} = 6.28$, $P = 0.020$, $P\eta^2 = 0.22$] which persisted after extinction [$F_{1,\ 22} = 6.31$, $P = 0.020$, $P\eta^2 = 0.22$; Fig. 3C]. A similar progressive differentiation across blocks was found for functional connectivity between amygdala and FFA [$F_{1,\ 22} = 5.70$, $P = 0.026$, $P\eta^2 = 0.21$], although here only the postextinction increase was significantly associated with spontaneous recovery [$F_{1,\ 22} = 8.0$, $P = 0.010$, $P\eta^2 = 0.27$]. Amygdala–hippocampus and amygdala–FFA connectivity furthermore did not differ between groups at baseline (block R1; both $F < 1$, n.s.). No differential increases were found for amygdala–vmPFC, amygdala–dACC, or amygdala–V1 connectivity (all $F < 1$, n.s.). Results were furthermore similar when using Spearman's rank order correlations instead of a median split for associations with spontaneous recovery (see Supplementary Results). Thus, stronger increases particularly in amygdala–hippocampal connectivity after acquisition predict spontaneous recovery on day 2, and these stronger increases persist after extinction.

The associations between resting-state connectivity increases on day 1 and spontaneous recovery on day 2 remained significant when covarying measures of sympathetic arousal during acquisition (conditioned pupil dilation to CS+ vs. CS− during acquisition, or heart rate frequency during acquisition or subsequent rest blocks). They also remained when controlling for connectivity strength during the acquisition phase. None of these covariates furthermore correlated with the observed increases in resting-state functional connectivity. To further examine whether these connectivity increases specifically predict recovery of the expression of differential conditioned fear (CS+ > CS−) and not broader contextual fear learning, we tested whether connectivity changes would also predict the differential autonomic response (change in average heart rate across blocks) to CS presentation blocks versus resting-state blocks on day 2, but this was not the case ($F < 1$, n.s., for amygdala connectivity with both hippocampus and FFA).

Intraregional Correlation Structures During Awake Rest Blocks

To specifically address our hypothesis that neuronal assemblies involved in representing the fear memory association within the amygdala reactivate spontaneously during offline periods following learning, we adopted a method that closely resembles techniques used in rodent electrophysiology to quantify replay of experience-specific patterns of neuronal firing (Qin et al. 1997; Kudrimoti et al. 1999; Lansink et al. 2008). We first calculated intra-amygdalar MVCS (Tambini and Davachi 2013) for each 4.5-min block by calculating the correlation between each voxel's time course and the time course of every other voxel within the amygdala (Fig. 4A). We then reasoned that if a specific set of distributed voxels that is activated during learning reactivates spontaneously during postlearning rest, a significant amount of variance in the MVCS after learning (e.g., in blocks R3–9) should be explained by variance in the MVCS sampled during learning (block A1), even when factoring out the correlation structure before learning (the MVCS for block R1). Evidence for such a correlation structure reactivation would be obtained if this EV is larger than the REV, that is, when pre- and postlearning estimates of the MVCS are exchanged (Lansink et al. 2008).

Results for this analysis are summarized in Figure 4B. Separate graphs are shown for participants who exhibit strong spontaneous recovery on day 2 and those who do not. Data for day 1 were analyzed using an rmANOVA with block (R3–6), hemisphere, and EV direction (EV vs. REV) as within-subject factors and spontaneous recovery as between-subjects factor. We observed a robust main effect of EV direction (EV > REV): $F_{1,\ 22} = 14.49$, $P = 0.001$, $P\eta^2 = 0.40$. Furthermore, this main effect was qualified by an interaction with the spontaneous recovery group factor [$F_{1,\ 22} = 4.38$, $P = 0.048$, $P\eta^2 = 0.17$], with stronger reactivation (EV > REV) in participants who showed stronger retention of fear memory on day 2. Further testing revealed a significant EV > REV effect in the strong spontaneous recovery group [$F_{1,\ 11} = 16.24$, $P = 0.002$, $P\eta^2 = 0.60$] but not in the weak recovery group [EV > REV: $F_{1,\ 11} = 1.58$, n.s.]. The EV > REV main effect [$F_{1,\ 22} = 14.8$, $P < 0.001$, $P\eta^2 = 0.40$] and the interaction with spontaneous recovery [$F_{1,\ 22} = 6.27$, $P = 0.020$, $P\eta_2 = 0.22$] reached significance already during postacquisition blocks (R3–4; Fig. 4B). No interactions with block (R3–6) or hemisphere were found.

If amygdala activation serves to reactivate a conjunctive representation linking the amygdala-dependent CS–UCS association to its spatiotemporal context (Rudy et al. 2004), then similar effects might be found in the hippocampus. We indeed found a main effect of EV direction (EV > REV) for hippocampus on day 1 [$F_{1,\ 22} = 15.47$, $P = 0.001$, $P\eta^2 = 0.41$; Fig. 5]. Similar to MVCS analyses for the amygdala, this main effect was also qualified by an interaction with spontaneous recovery group [$F_{1,\ 22} = 5.94$, $P = 0.023$, $P\eta^2 = 0.21$]. Further testing revealed a robust reactivation (EV > REV) effect in the strong spontaneous recovery group [$F_{1,\ 11} = 11.84$, $P = 0.006$, $P\eta_2 = 0.52$], but only a near-significant trend in the weak recovery group [$F_{1,\ 11} = 3.91$, $P = 0.074$, $P\eta^2 = 0.26$]. No main effects or interactions involving the factor block were found. During postacquisition blocks (R3–4), the EV > REV effect already reached significance [$F_{1,\ 22} = 23.29$, $P < 0.001$, $P\eta^2 = 0.51$], while the interaction with spontaneous recovery yielded a trend [$F_{1,\ 22} = 3.12$, $P = 0.09$, $P\eta^2 = 0.12$]. On day 2, reactivation (EV > REV) was again stronger in the strong spontaneous recovery group [EV direction by spontaneous recovery group interaction: $F_{1,\ 23} = 5.53$, $P = 0.028$, $P\eta^2 = 0.20$; EV > REV effect in strong spontaneous recovery group: $F_{1,\ 11} = 4.16$, $P = 0.066$, $P\eta^2 = 0.27$; no EV > REV effect in the weak recovery group].

Reactivation (EV > REV) measures for amygdala and hippocampus were correlated across participants ($r(22) = 0.76$, $P < 0.001$) but were not associated with measures of arousal, differential conditioning, functional connectivity during acquisition, regional volume, or the differential autonomic responses (change in average heart rate across blocks) to CS presentation blocks versus resting-state blocks on day 2. The pattern of results linking these reactivation measures to spontaneous recovery of fear on day 2 furthermore did not change after covarying these measures. Results were furthermore similar when using Spearman's rank order correlations instead of median split for associations with spontaneous recovery (see Supplementary Results). Finally, a control analysis on data sampled from V1 yielded evidence for neither an EV > REV effect [$F_{1,\ 22} = 3.10$, n.s.], nor an association with spontaneous recovery ($F < 1$, n.s.).

Discussion

This study aimed to investigate neural mechanisms underlying consolidation of fear memory by tracking changes in interregional functional connectivity and persistence of intraregional multi-

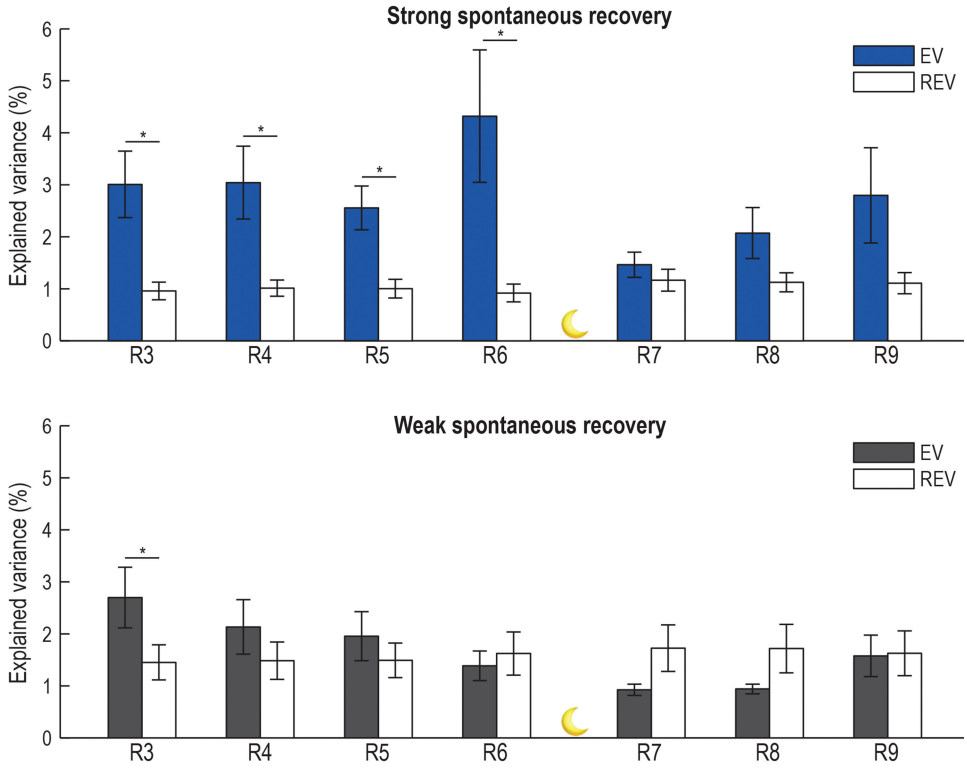

Figure 5. Intraregional multi-voxel connectivity structure analysis on hippocampus. EV and REV are plotted for bilateral hippocampus, separately for each resting-state block after fear learning (R3–9) and group (strong spontaneous recovery vs. weak spontaneous recovery). EV, explained variance; REV, reverse explained variance; *EV > REV, $P < 0.05$.

voxel patterns following fear learning and extinction. We found postlearning increases in functional connectivity of the amygdala primarily with the hippocampus, but also with vmPFC, FFA, and V1. We found no significant increase for dACC, a region known to be activated during expression of fear (Milad and Quirk 2012). Second, we show that within the amygdala and hippocampus, a voxel-pairwise correlation structure sampled during the first block of fear acquisition is reinstated spontaneously during postacquisition rest. Third, postacquisition functional connectivity between amygdala and hippocampus, as well as reinstatement of multi-voxel patterns within these regions, persisted after extinction and was stronger in participants who exhibited long-term expression of the fear memory as reflected in spontaneous recovery of conditioned fear 1 day later.

In a 2-day paradigm involving acquisition and extinction on day 1 and re-extinction on day 2, we observed a recovery of the differential fear response in a subset of participants on day 2. Similar paradigms combining extinction with delayed recall have proven fruitful in discovering factors that influence long-term expression and recovery of fear, such as disruption of reconsolidation (Kindt et al. 2009; Schiller et al. 2010; 2013), individual differences in brain structure (Hartley et al. 2011), and pharmacological manipulation during extinction (Haaker et al. 2013). Models of extinction learning postulate that extinction does not overwrite the original fear memory, but creates a novel safety association that competes with the original fear memory and is supported by distinct neural systems (Bouton 2002; Milad and Quirk 2012). A limitation of designs such as the one employed in the present study is therefore that spontaneous recovery of a previously extinguished fear response can be due to either strong retention of the original fear memory or to poor retention of the extinction memory. A functional interpretation of neural measures that predict spontaneous recovery therefore has to rely on prior knowledge of the functions (fear learning versus extinction) of the neural circuits involved.

Analyses of interregional functional connectivity revealed robust coupling between amygdala and hippocampus. This finding concurs with anatomical studies in rodents showing dense bidirectional interconnections between these regions, in particular between the basolateral regions of the amygdala and various regions within the hippocampal complex, including CA1, CA3, and entorhinal cortex (Pitkänen et al. 2000). In humans, resting functional connectivity between amygdala and hippocampus has been shown using BOLD-fMRI (Roy et al. 2009). We extend these findings by showing that amygdala–hippocampal coupling increases progressively during postlearning rest. Amygdala–hippocampal connectivity is not just proportional to time spent in the scanner, because functional connectivity decreases over time during later acquisition/extinction blocks (see Supplementary Fig. 3). It is also not merely driven by exposure to faces, because it decreases during blocks in which participants are exposed to these stimuli. Our finding aligns closely with electrophysiological studies in rodents, which have shown increased synchronized theta-band oscillations between LA and CA1 after fear conditioning (Seidenbecher et al. 2003). Interactions between LA and CA1 were furthermore shown to increase rapidly after exposure to immobilization stress (Ghosh et al. 2013). The relationship between slow BOLD-fMRI fluctuations (0.01–0.1 Hz) observed in humans and oscillations in theta (4–14 Hz) and higher frequency bands observed using intracranial recordings in rodents remains unclear. However, there is growing consensus that BOLD fluctuations reflect slow fluctuations in the band-

limited power envelope of higher frequency oscillations (Liu et al. 2010).

Amygdala–hippocampal connectivity during both postacquisition and postextinction blocks increased more strongly for participants who exhibited spontaneous recovery on day 2. This finding corresponds with the observation that rodents with stronger increases in synchronization of theta-band oscillations between (B) LA and hippocampus during paradoxical sleep after fear learning exhibits stronger fear memory retention (Popa et al. 2010), but extends these findings to awake rest. In humans, enhanced connectivity between amygdala and (para) hippocampal regions has been shown during formation (Dolcos et al. 2004) and retrieval (Smith et al. 2006) of episodic memory for emotional events. Moreover, amygdala lesions block enhanced hippocampal activity during emotional memory formation (Richardson et al. 2004). An interpretation of our finding in terms of a lack of extinction retention does not appear plausible, because substantial evidence shows that extinction retention depends on amygdala–vmPFC circuits (Milad and Quirk 2012), and we do not find an association between amygdala–vmPFC connectivity and spontaneous recovery. We therefore conclude that our findings lend support to the hypothesis that amygdala–hippocampal coupling underlies enhanced retention of fear memory, a core assumption of models of emotional memory consolidation (Phelps 2004; Roozendaal et al. 2009; Pape and Paré 2010; Hermans et al. 2014). Our findings further show that enhanced amygdala–hippocampal coupling persists despite the fact that expression of the fear memory is suppressed following extinction.

We found a similar progressive increase in connectivity between amygdala and FFA, which was also associated with stronger spontaneous recovery on day 2. As a region involved in processing facial features (Kanwisher et al. 1997), FFA is likely necessary to represent distinguishing features of the facial CS that was linked to shock. Fear learning is known to cause lasting changes in sensitivity of cortical regions that represent sensory features of conditioned stimuli (Weinberger 1998; Apergis-Schoute et al. 2014). Our findings suggest that such representations may be strengthened through repeated reactivations after learning (Frankland and Bontempi 2005; Tambini et al. 2010).

Within the amygdala, we found that a structure of multivoxel pairwise correlations sampled during the first fear learning block persisted during postlearning rest. This MVCS reinstatement cannot be explained by patterns of underlying structural connectivity, because we controlled for correlation structures present prior to learning (cf. Lansink et al. 2008). Our findings, therefore, indicate that a specific subset of distributed voxels within the amygdala that co-activates during the fear acquisition block reactivates spontaneously during postlearning rest. This finding is consistent with observations in rodents that CS–US associations are sparsely coded across distributed neuronal assemblies within the BLA (Reijmers et al. 2007), and that BLA neurons exhibit prolonged increases in firing rates following emotional arousal (Pelletier et al. 2005). Specific subsets of BLA neurons have furthermore been shown to be involved in the modulatory effect of the BLA on the hippocampus (Paré 2003; Roozendaal et al. 2009). Activation of such distributed neuronal populations, possibly accompanied by inhibition of surrounding neurons, may result in shifts in patterns of BOLD that can be detected using multivariate techniques such as the MVCS analysis employed in the present study. Our observation that postlearning reactivations of these MVCSs predict spontaneous recovery of fear on day 2 establishes a correlational link of MVCS reinstatement with long-term expression of the fear memory, which is in line with trace-reactivation accounts of memory consolidation (Wilson and McNaughton 1994; Rasch and Born 2007).

It should be noted, however, that the MVCSs were sampled across the entire block of fear acquisition, which included both CS+ and CS– presentations, and intertrial intervals. The MVCSs may therefore contain synchronized activity that is not time locked to CS presentations and is not directly related to the convergence of information regarding the CS and the US. A potential solution to this problem would be to sample event-related response patterns evoked by the CS+. A number of previous studies have employed such an approach (Bach et al. 2011; Visser et al. 2011, 2013; Dunsmoor et al. 2014). However, these studies compared such evoked response patterns with other evoked response patterns, while our goal was to detect reinstatements of learning patterns that are unpredictable in time, which greatly reduces power. The advantage of the MVCS approach used here over other forms of multi-voxel pattern analysis is that the MVCS is insensitive to this temporal unpredictability, because a simultaneous activation in 2 given voxels increases the temporal correlation between these voxels regardless of when this coactivation takes place (Tambini and Davachi 2013). Nonetheless, future work is necessary to establish the specificity of reactivations to representations of conditioned stimuli.

One alternative explanation for the observed MVCS reinstatement effect is that it reflects a persistence of unspecific arousal. Although neural circuits subserving fear learning and those controlling arousal are intricately linked in the amygdala (Fendt and Fanselow 1999), an interpretation of the MVCS reinstatement effect in terms of reactivation of the fear memory association would be problematic if arousal alone would explain this effect. However, our analyses show that this is not the case. Strength of postlearning MVCS reinstatement did not correlate with strength of conditioned pupil dilation, conditioned SCR magnitudes, or heart rate frequency. Spontaneous recovery of fear on day 2 was furthermore not associated with any of these measures of arousal, and all effects remained after controlling for arousal. Therefore, although arousal-related processes are likely to be involved, the postlearning MVCS reinstatement cannot be explained only by persistent arousal.

Another possible explanation is that the observed postlearning MVCS reinstatement is driven by other cognitive processes such as relational or contextual processing. This interpretation appears implausible when only considering the amygdala, because unlike cue conditioning (Miserendino et al. 1990; Rogan et al. 1997; Pape and Paré 2010), contextual memory does not depend on this region (Bechara et al. 1995; Labar and Cabeza 2006). However, we found persistence of MVCSs also in the hippocampus, which is thought to support the formation of a conjunctive representation of a fear cue and its spatiotemporal context (Kim and Fanselow 1992; Rudy et al. 2004). This observation closely resembles recent findings of post-encoding persistence of hippocampal MVCSs related to associative memory formation in humans (Tambini and Davachi 2013). Although BOLD-fMRI cannot approach the same level of spatiotemporal detail, such findings are in line with electrophysiological studies in rodents showing replay of neuronal spiking patterns in hippocampal cell assemblies involved in representing spatial context (Moser et al. 2008). This phenomenon has been observed during both postlearning sleep (Pavlides and Winson 1989; Wilson and McNaughton 1994; Skaggs and McNaughton 1996; Kudrimoti et al. 1999) and postlearning waking states (Kudrimoti et al. 1999; Carr et al. 2011; Atherton et al. 2015). Awake replay is

furthermore enhanced following salient experiences (Cheng and Frank 2008; Karlsson and Frank 2009), and selective disruption of replay by blocking neuronal activity during hippocampal sharp-wave ripples negatively affects later memory (Girardeau et al. 2009; Ego-Stengel and Wilson 2010; Jadhav et al. 2012). In the present study, postlearning MVCS reinstatement effects in amygdala and hippocampus were highly correlated, and connectivity between these 2 regions increased after fear learning. Although we did not find evidence that these postlearning changes were predictive of the autonomic response (heart rate change) to CS presentation blocks versus rest blocks, which could be seen as a measure of contextual fear, it appears plausible that reactivation of circuits involved in fear learning coincide with reactivation of a broader associative network including representations of the spatiotemporal context in which fear learning took place. Such coactivation may also explain why hippocampal MVCS reinstatement correlated with spontaneous recovery despite the fact that cue conditioning does not depend on the hippocampus (Bechara et al. 1995).

Our findings add to a growing body of human evidence linking systems-level interactions in the immediate postencoding time window to subsequent memory strength (Tambini et al. 2010; Staresina et al. 2013; Tambini and Davachi 2013). An important question is whether the observed postlearning interactions within and between amygdala and hippocampus indeed contribute causally to consolidation or whether these findings reflect persistent activity that is carried over from encoding but does not functionally contribute to memory consolidation. Speaking against this latter possibility, activity in amygdala and hippocampus observed during fear learning (cf. Buchel et al. 1999; Phelps et al. 2004) did not predict spontaneous recovery on day 2. Stronger post-encoding activity therefore does not solely reflect persistence of activity that was already elevated during encoding. It should be noted that the observed increase in postlearning functional connectivity indicates the presence of enhanced synchronized slow (0.01–0.1 Hz) BOLD signal fluctuations. The present results thus agree with observations in rodents that reactivations of mnemonic representations after learning involve fluctuating ensemble activity rather than a fixed activity state (Hoffman and McNaughton 2002).

A final critical question is whether correlations of post-encoding activity with later memory strength are observed, because interactions in the immediate phase are representative of a stable process that unfolds over a longer time window. This interpretation would be consistent with animal models of systems consolidation, which assume that systems consolidation is a slow process of transformation of memory traces (Frankland and Bontempi 2005). Another possibility is that neural interactions during the first minutes after encoding serve a distinct function. For instance, awake reactivations of recent memories have been suggested to promote adaptive memory updating (Carr et al. 2011). Answering this question will require studies tracking and causally manipulating the time course of systems-level interactions during consolidation.

In conclusion, we demonstrate that neural circuits activated during fear learning exhibit persistent activity during postacquisition as well as postextinction rest that predicts long-term expression of the fear memory. This finding lends tentative support to accounts of long-term memory formation that assume a role for spontaneous reactivations of neural representations of recent experiences in the process of consolidation (Wilson and McNaughton 1994; Paré 2003; Rasch and Born 2007; Pape and Paré 2010).

Supplementary Material

Supplementary material can be found at: http://www.cercor.oxfordjournals.org/online.

Funding

This work was supported by the Netherlands Organisation for Scientific Research (grant number 451.07.019 to E.J.H.) and the National Institutes of Health (grant number MH080756 to E.A.P.).

Notes

Conflict of Interest: None declared.

References

Albert NB, Robertson EM, Miall RC. 2009. The resting human brain and motor learning. Curr Biol. 19:1023–1027.

Andersson JLR, Skare S, Ashburner J. 2003. How to correct susceptibility distortions in spin-echo echo-planar images: application to diffusion tensor imaging. NeuroImage. 20:870–888.

Apergis-Schoute AM, Schiller D, LeDoux JE, Phelps EA. 2014. Extinction resistant changes in the human auditory association cortex following threat learning. Neurobiol Learn Mem. 113:109–114.

Ashburner J. 2007. A fast diffeomorphic image registration algorithm. NeuroImage. 38:95–113.

Ashburner J, Friston KJ. 2005. Unified segmentation. NeuroImage. 26:839–851.

Atherton LA, Dupret D, Mellor JR. 2015. Memory trace replay: the shaping of memory consolidation by neuromodulation. Trends Neurosci. 38:560–570.

Bach DR, Weiskopf N, Dolan RJ. 2011. A stable sparse fear memory trace in human amygdala. J Neurosci. 31:9383–9389.

Bechara A, Tranel D, Damasio H, Adolphs R, Rockland C, Damasio AR. 1995. Double dissociation of conditioning and declarative knowledge relative to the amygdala and hippocampus in humans. Science. 269:1115–1118.

Bouton ME. 2002. Context, ambiguity, and unlearning: sources of relapse after behavioral extinction. Biol Psychiatry. 52:976–986.

Buchel C, Dolan RJ, Armony JL, Friston KJ. 1999. Amygdala-hippocampal involvement in human aversive trace conditioning revealed through event-related functional magnetic resonance imaging. J Neurosci. 19:10869–10876.

Carr MF, Jadhav SP, Frank LM. 2011. Hippocampal replay in the awake state: a potential substrate for memory consolidation and retrieval. Nat Neurosci. 14:147–153.

Cheng S, Frank LM. 2008. New experiences enhance coordinated neural activity in the hippocampus. Neuron. 57:303–313.

Dolcos F, Labar KS, Cabeza R. 2004. Interaction between the amygdala and the medial temporal lobe memory system predicts better memory for emotional events. Neuron. 42:855–863.

Dunsmoor JE, Kragel PA, Martin A, Labar KS. 2014. Aversive learning modulates cortical representations of object categories. Cereb Cortex. 24:2859–2872.

Dunsmoor JE, Niv Y, Daw N, Phelps EA. 2015. Rethinking extinction. Neuron. 88:47–63.

Ego-Stengel V, Wilson MA. 2010. Disruption of ripple-associated hippocampal activity during rest impairs spatial learning in the rat. Hippocampus. 20:1–10.

Fendt M, Fanselow MS. 1999. The neuroanatomical and neurochemical basis of conditioned fear. Neurosci Biobehav Rev. 23:743–760.

Feng T, Feng P, Chen Z. 2013. Altered resting-state brain activity at functional MRI during automatic memory consolidation of fear conditioning. Brain Res. 1523:59–67.

Frankland PW, Bontempi B. 2005. The organization of recent and remote memories. Nat Rev Neurosci. 6:119–130.

Ghosh S, Laxmi TR, Chattarji S. 2013. Functional connectivity from the amygdala to the hippocampus grows stronger after stress. J Neurosci. 33:7234–7244.

Girardeau G, Benchenane K, Wiener SI, Buzsáki G, Zugaro MB. 2009. Selective suppression of hippocampal ripples impairs spatial memory. Nat Neurosci. 12:1222–1223.

Glover GH, Li TQ, Ress D. 2000. Image-based method for retrospective correction of physiological motion effects in fMRI: RETROICOR. Magn Reson Med. 44:162–167.

Haaker J, Gaburro S, Sah A, Gartmann N, Lonsdorf TB, Meier K, Singewald N, Pape HC, Morellini F, Kalisch R. 2013. Single dose of L-dopa makes extinction memories context-independent and prevents the return of fear. Proc Natl Acad Sci USA. 110:E2428–E2436.

Hartley CA, Fischl B, Phelps EA. 2011. Brain structure correlates of individual differences in the acquisition and inhibition of conditioned fear. Cereb Cortex. 21:1954–1962.

Hasson U, Nusbaum HC, Small SL. 2009. Task-dependent organization of brain regions active during rest. Proc Natl Acad Sci USA. 106:10841–10846.

Hermans EJ, Battaglia FP, Atsak P, de Voogd LD, Fernández G, Roozendaal B. 2014. How the amygdala affects emotional memory by altering brain network properties. Neurobiol Learn Mem. 112:2–16.

Hermans EJ, Henckens MJAG, Roelofs K, Fernández G. 2013. Fear bradycardia and activation of the human periaqueductal grey. NeuroImage. 66:278–287.

Hoffman KL, McNaughton BL. 2002. Coordinated reactivation of distributed memory traces in primate neocortex. Science. 297:2070–2073.

Jadhav SP, Kemere C, German PW, Frank LM. 2012. Awake hippocampal sharp-wave ripples support spatial memory. Science. 336:1454–1458.

Kanwisher N, McDermott J, Chun MM. 1997. The fusiform face area: a module in human extrastriate cortex specialized for face perception. J Neurosci. 17:4302–4311.

Karlsson MP, Frank LM. 2009. Awake replay of remote experiences in the hippocampus. Nat Neurosci. 12:913–918.

Kim JJ, Fanselow MS. 1992. Modality-specific retrograde amnesia of fear. Science. 256:675–677.

Kindt M, Soeter M, Vervliet B. 2009. Beyond extinction: erasing human fear responses and preventing the return of fear. Nat Neurosci. 12:256–258.

Kudrimoti HS, Barnes CA, McNaughton BL. 1999. Reactivation of hippocampal cell assemblies: effects of behavioral state, experience, and EEG dynamics. J Neurosci. 19:4090–4101.

Labar KS, Cabeza R. 2006. Cognitive neuroscience of emotional memory. Nat Rev Neurosci. 7:54–64.

LaBar KS, Gatenby JC, Gore JC, LeDoux JE, Phelps EA. 1998. Human amygdala activation during conditioned fear acquisition and extinction: a mixed-trial fMRI study. Neuron. 20:937–945.

LaBar KS, Phelps EA. 1998. Arousal-mediated memory consolidation: role of the medial temporal lobe in humans. Psych Sci. 9:490–493.

Lansink CS, Goltstein PM, Lankelma JV, Joosten RNJMA, McNaughton BL, Pennartz CMA. 2008. Preferential reactivation of motivationally relevant information in the ventral striatum. J Neurosci. 28:6372–6382.

Lewis CM, Baldassarre A, Committeri G, Romani GL, Corbetta M. 2009. Learning sculpts the spontaneous activity of the resting human brain. Proc Natl Acad Sci USA. 106:17558–17563.

Liu Z, Fukunaga M, de Zwart JA, Duyn JH. 2010. Large-scale spontaneous fluctuations and correlations in brain electrical activity observed with magnetoencephalography. NeuroImage. 51:102–111.

Lundqvist D, Flykt A, Ohman A. 1998. The Karolinska directed emotional faces. Stockholm: Karolinska Institute.

McGaugh JL. 2000. Memory—a century of consolidation. Science. 287:248–251.

Milad MR, Quirk GJ. 2002. Neurons in medial prefrontal cortex signal memory for fear extinction. Nature. 420:70–74.

Milad MR, Quirk GJ. 2012. Fear extinction as a model for translational neuroscience: ten years of progress. Annu Rev Psychol. 63:129–151.

Miserendino MJ, Sananes CB, Melia KR, Davis M. 1990. Blocking of acquisition but not expression of conditioned fear-potentiated startle by NMDA antagonists in the amygdala. Nature. 345:716–718.

Moser EI, Kropff E, Moser M-B. 2008. Place cells, grid cells, and the brain's spatial representation system. Annu Rev Neurosci. 31:69–89.

Pape H-C, Paré D. 2010. Plastic synaptic networks of the amygdala for the acquisition, expression, and extinction of conditioned fear. Physiol Rev. 90:419–463.

Paré D. 2003. Role of the basolateral amygdala in memory consolidation. Prog Neurobiol. 70:409–420.

Pavlides C, Winson J. 1989. Influences of hippocampal place cell firing in the awake state on the activity of these cells during subsequent sleep episodes. J Neurosci. 9:2907–2918.

Pelletier JG, Likhtik E, Filali M, Paré D. 2005. Lasting increases in basolateral amygdala activity after emotional arousal: implications for facilitated consolidation of emotional memories. Learn Mem. 12:96–102.

Phelps EA. 2004. Human emotion and memory: interactions of the amygdala and hippocampal complex. Curr Opin Neurobiol. 14:198–202.

Phelps EA, Delgado MR, Nearing KI, LeDoux JE. 2004. Extinction learning in humans: role of the amygdala and vmPFC. Neuron. 43:897–905.

Pitkänen A, Pikkarainen M, Nurminen N, Ylinen A. 2000. Reciprocal connections between the amygdala and the hippocampal formation, perirhinal cortex, and postrhinal cortex in rat. A review. Ann N Y Acad Sci. 911:369–391.

Popa D, Duvarci S, Popescu AT, Léna C, Paré D. 2010. Coherent amygdalocortical theta promotes fear memory consolidation during paradoxical sleep. Proc Natl Acad Sci USA. 107: 6516–6519.

Poulos AM, Li V, Sterlace SS, Tokushige F, Ponnusamy R, Fanselow MS. 2009. Persistence of fear memory across time requires the basolateral amygdala complex. Proc Natl Acad Sci USA. 106:11737–11741.

Qin YL, McNaughton BL, Skaggs WE, Barnes CA. 1997. Memory reprocessing in corticocortical and hippocampocortical neuronal ensembles. Phil Trans R Soc B. 352:1525–1533.

Rasch B, Born J. 2007. Maintaining memories by reactivation. Curr Opin Neurobiol. 17:698–703.

Reijmers LG, Perkins BL, Matsuo N, Mayford M. 2007. Localization of a stable neural correlate of associative memory. Science. 317:1230–1233.

Reinders AATS, Boer den JA, Buchel C. 2005. The robustness of perception. Eur J Neurosci. 22:524–530.

Reinhard G, Lachnit H. 2002. Differential conditioning of anticipatory pupillary dilation responses in humans. Biol Psychol. 60:51–68.

Richardson MP, Strange BA, Dolan RJ. 2004. Encoding of emotional memories depends on amygdala and hippocampus and their interactions. Nat Neurosci. 7:278–285.

Rissman J, Wagner AD. 2012. Distributed representations in memory: insights from functional brain imaging. Annu Rev Psychol. 63:101–128.

Rogan MT, Stäubli UV, LeDoux JE. 1997. Fear conditioning induces associative long-term potentiation in the amygdala. Nature. 390:604–607.

Roozendaal B, McEwen BS, Chattarji S. 2009. Stress, memory and the amygdala. Nat Rev Neurosci. 10:423–433.

Roy AK, Shehzad Z, Margulies DS, Kelly AMC, Uddin LQ, Gotimer K, Biswal BB, Castellanos FX, Milham MP. 2009. Functional connectivity of the human amygdala using resting state fMRI. NeuroImage. 45:614–626.

Rudy JW, Huff NC, Matus-Amat P. 2004. Understanding contextual fear conditioning: insights from a two-process model. Neurosci Biobehav Rev. 28:675–685.

Schiller D, Kanen JW, LeDoux JE, Monfils MH, Phelps EA. 2013. Extinction during reconsolidation of threat memory diminishes prefrontal cortex involvement. Proc Natl Acad Sci USA. 110:20040–20045.

Schiller D, Monfils M-H, Raio CM, Johnson DC, LeDoux JE, Phelps EA. 2010. Preventing the return of fear in humans using reconsolidation update mechanisms. Nature. 463: 49–53.

Schultz DH, Balderston NL, Helmstetter FJ. 2012. Resting-state connectivity of the amygdala is altered following Pavlovian fear conditioning. Front Hum Neurosci. 6:242.

Seidenbecher T, Laxmi TR, Stork O, Pape H-C. 2003. Amygdalar and hippocampal theta rhythm synchronization during fear memory retrieval. Science. 301:846–850.

Siegle G. 2003. Use of concurrent pupil dilation assessment to inform interpretation and analysis of fMRI data. NeuroImage. 20:114–124.

Skaggs WE, McNaughton BL. 1996. Replay of neuronal firing sequences in rat hippocampus during sleep following spatial experience. Science. 271:1870–1873.

Smith APR, Stephan KE, Rugg MD, Dolan RJ. 2006. Task and content modulate amygdala-hippocampal connectivity in emotional retrieval. Neuron. 49:631–638.

Staresina BP, Alink A, Kriegeskorte N, Henson RN. 2013. Awake reactivation predicts memory in humans. Proc Natl Acad Sci USA. 110:21159–21164.

Tambini A, Davachi L. 2013. Persistence of hippocampal multivoxel patterns into postencoding rest is related to memory. Proc Natl Acad Sci USA. 110:19591–19596.

Tambini A, Ketz N, Davachi L. 2010. Enhanced brain correlations during rest are related to memory for recent experiences. Neuron. 65:280–290.

Thomason ME, Burrows BE, Gabrieli JDE, Glover GH. 2005. Breath holding reveals differences in fMRI BOLD signal in children and adults. NeuroImage. 25:824–837.

Tzourio-Mazoyer N, Landeau B, Papathanassiou D, Crivello F, Etard O, Delcroix N, Mazoyer B, Joliot M. 2002. Automated anatomical labeling of activations in SPM using a macroscopic anatomical parcellation of the MNI MRI single-subject brain. NeuroImage. 15:273–289.

Van Dijk KRA, Hedden T, Venkataraman A, Evans KC, Lazar SW, Buckner RL. 2010. Intrinsic functional connectivity as a tool for human connectomics: theory, properties, and optimization. J Neurophysiol. 103:297–321.

van Kesteren MTR, Fernández G, Norris DG, Hermans EJ. 2010. Persistent schema-dependent hippocampal-neocortical connectivity during memory encoding and postencoding rest in humans. Proc Natl Acad Sci USA. 107:7550–7555.

van Marle HJF, Hermans EJ, Qin S, Fernández G. 2010. Enhanced resting-state connectivity of amygdala in the immediate aftermath of acute psychological stress. NeuroImage. 53: 348–354.

Visser RM, Scholte HS, Beemsterboer T, Kindt M. 2013. Neural pattern similarity predicts long-term fear memory. Nat Neurosci. 16:388–390.

Visser RM, Scholte HS, Kindt M. 2011. Associative learning increases trial-by-trial similarity of BOLD-MRI patterns. J Neurosci. 31:12021–12028.

Wegman J, Janzen G. 2011. Neural encoding of objects relevant for navigation and resting state correlations with navigational ability. J Cogn Neurosci. 23:3841–3854.

Weinberger NM. 1998. Physiological memory in primary auditory cortex: characteristics and mechanisms. Neurobiol Learn Mem. 70:226–251.

Wilson MA, McNaughton BL. 1994. Reactivation of hippocampal ensemble memories during sleep. Science. 265:676–679.